Epifluorescence Studies and Secondary Relaxation Processes in Immiscible Blends of Polybutadiene-Poly(2-vinyl naphthalene) by Fluorescence Spectroscopy

M. C. P. CRUZ, F. M. CASSIOLA, T. D. Z. ATVARS

Instituto de Química, Caixa Postal 6154, CEP 13083-970 Campinas, SP, Brazil

Received 27 February 2001; accepted 5 June 2001

ABSTRACT: The development of the morphology of polybutadiene/poly(2-vinyl naphthalene) blends in five proportions by mass (5, 10, 50, 90, and 95%, w/w) is studied by epifluorescence and scanning electron microscopy (SEM) techniques. The phase separation process of these immiscible polymers produces a primary morphology that is formed by dispersed droplets in a continuous matrix. In the sequence a secondary phase separation inside the primary domains is detected by epifluorescence microscopy of the intrinsically fluorescent domains. Secondary phase separation is confirmed by SEM fracture surface analysis. The relative size of the droplets and the matrix composition depend on the proportion of the components of the blends. The mechanism of the phase separation process is preferentially by nucleation growth for either primary or secondary phase separation processes. Secondary relaxation processes involving the poly(2-vinyl naphthalene) phase are studied by fluorescence spectroscopy. The profile of the steady-state excimer fluorescence of poly(2-vinyl naphthalene) with the temperature in the blend differs from that of the isolated homopolymer and is explained by the contribution from the interface to the radiationless deactivation. The Arrhenius plot for the temperature dependence exhibits slope changes that are related to the polymer relaxation processes. © 2002 Wiley Periodicals, Inc. J Appl Polym Sci 84: 1637–1649, 2002; DOI 10.1002/app.10389

Key words: epifluorescence microscopy; polybutadiene; poly(2-vinyl naphthalene); relaxation processes; scanning electron microscopy

INTRODUCTION

Studies of polymer blends may be considered from different viewpoints. In some cases optimization of properties is the main interest and in others compatibilization of the phases or preparation of a miscible material is emphasized. Regardless of the aim of the work, the final properties and morphology of the material are controlled by the interfacial properties. Nevertheless, the determination of the interfacial properties in microheterogeneous materials, including polymer blends, is still difficult, regardless of whether we consider theoretical models or experimental methodology. The main reasons for these difficulties reside in the width of the interface and in the absence of precise thermodynamic models describing the gradient of composition throughout the interfacial cross section.[1–5] In immiscible polymer blends the interfacial tension increases with the molecular weight of each homopolymer and linearly decreases with the increase of the temperature.[4]

Direct study of polymer interfaces is a very difficult task, and measurements of composition

Correspondence to: T. D. Z. Atvars (tatvars@iqm.unicamp.br).

Contract grant sponsor: FAPESP.

Journal of Applied Polymer Science, Vol. 84, 1637–1649 (2002)

profiles across the interface have not been achieved. Several techniques are currently employed, such as different types of microscopy, scattering techniques (light, neutron, X-ray, ion), IR spectroscopy, and X-ray microanalysis.[3] Measurements involving small angle X-ray scattering, small angle neutron scattering, and nonradiative energy transfer processes demonstrated that an interface thickness is typically about 3 nm.[5–7]

Luminescence studies were successfully applied for the evaluation of polymer blend miscibility at the limit of the molecular scale.[8–11] Several of these studies were based on two general approaches: the measurements of the excimer/monomer ratio and its relationship with polymer miscibility and the determination of the efficiency of the radiationless energy transfer processes that are dependent on polymer interpenetration and thus with polymer miscibility. Moreover, luminescence techniques have also been successfully applied in studies of polymer, copolymer, and polymer blend relaxation processes.[12–22] Usually, the studies of the relaxation processes of polymeric materials using luminescence techniques can be performed using steady-state or time-resolved emission spectroscopy.[21] If the system is not intrinsically luminescent, a luminescent guest sorbed in the material can be employed or the polymer can be chemically modified by the addition of a luminescent chromophore chemically bonded to the chain.[22–24]

Several types of microscopy techniques were successfully used to determine the morphology of polymer blends and, in particular, epifluorescence microscopy revealed the composition distribution of the fluorophore in phase separated domains.[12–14,25] Nevertheless, quantitative measurements are still not possible.

The present work describes the morphology of polybutadiene/poly(2-vinyl naphthalene) (PB/P2VN) blends prepared by casting polymer solutions onto a glass surface in five different proportions by mass. The morphology is studied by epifluorescence complemented by electron scanning microscopy techniques. P2VN is an intrinsically fluorescent polymer that is very similar to polystyrene (PS), which is the most employed polymer, along with PB, for technological applications.[26] This polymer (P2VN) is chosen instead of PS because of its higher fluorescence quantum yield,[9,10] which allows easier observation of the morphology using a conventional epifluorescence microscope. As an analogue of PS, blends of P2VN with PB should also be immiscible with an upper critical solution temperature and we thus assume that the morphological properties might also be similar and that the results produced in this work can be transferred to the other polymeric system.[27–32] In addition, because the morphology of the PB/PS blend is also controlled by the PB microstructure, PB with a high content of 1-2-trans addition was chosen in the present work.[30]

We also report studies of the polymer relaxation processes using the steady-state fluorescence spectroscopy of P2VN. This study is based on measurements of the fluorescence spectra at several temperature, which is dependent on the intrinsic properties of the fluorescent group and the polymer relaxation processes of the material.[21]

EXPERIMENTAL

Materials and Preparation of Samples

The P2VN (Aldrich Chemical Co.) was used as received. The 1,4-*cis* PB (PB-36, Aldrich) was purified by exhaustive Sohxlet extraction for 40 h, using ethanol as a solvent. This purification process was followed by Fourier transform IR spectroscopy (FTIR). Dichoromethane (spectrophotometric grade, Merck) was used as received.

Polymer blend films were prepared by mixing stock dichloromethane solutions containing both homopolymers and casting the solutions onto a Petri dish. Homopolymer solutions were mixed to produce polymer blends with the desired proportions of PB-36/P2VN (0, 5, 10, 50, 90, 95, and 100 wt %). Films were dried at room temperature in air and then kept for a couple of weeks in a desiccator under a vacuum. Finally they were annealed at 80°C in an oven under a vacuum for 8 h and then kept at room temperature until measurement. The annealing process was considered crucial to stabilize the final morphology of the blends prepared by casting. No solvent residual was detected by thermal gravimetric analysis (TGA). The film thickness was 70–80 μm.

Characterization Techniques

Films of homopolymers and polymer blends were characterized by differential scanning calorimetry (DSC; model v2.2A 990, DuPont) that was calibrated with indium as a standard. Two scans were performed for every sample: the first scan heated the sample from room temperature to 150°C, the sample was then quenched (20°C/min)

Table I Physical Properties of PB-36 and P2VN Polymers

Physical Property	P2VN	PB-36
M_w (g mol^{-1})	59,000	203,208
Polydispersity	2.7	4.1
T_g (°C)	118	−89
Microstructure (FTIR)	—	14% vinyl, 50%-1,4-trans, 36%-1,4-cis units
T_d (°C)	350	260

T_d, the onset of the decomposition temperature as measured by thermal analysis.

to −150°C, and it was finally heated to 150°C. The heating rate was 10°C /min.

The molecular weight and molecular weight distributions of P2VN and PB-36 were determined by gel permeation chromatography (GPC) using a Waters chromatograph (model 486) with a model 410 refractive index detector and THF as the eluent at a temperature of 40°C; PS was used as the standard. Three coupled 7-μm Ultrastyragel (Waters) columns (7.8 × 300 mm) were employed for the size separation range of about 2 × 10^3 to 4 × 10^6 g mol^{-1}. Sample solutions were filtered (0.45 μm), and the filtered solution was injected into the chromatograph. Because PB-36 is partially soluble under these conditions, its molecular weight refers to its soluble fraction.

The microstructure of PB-36 was determined by IR spectroscopy using a Perkin–Elmer model 16PC FTIR spectrophotometer. The spectrum resolution was 2 cm^{-1} over the spectral range of 400–5000 cm^{-1} and using an accumulation of 102 scans. Data were collected and analyzed using standard software. Films of PB-36 were cast from a dichloromethane solution onto a KBr plate, and the IR spectra were measured using air as the background.

Epifluorescence microscopy was performed using a standard Zeiss Jena universal microscope. A dichroic mirror selects the excitation wavelength ($\lambda_{exc} < 380$ nm) of a mercury UV lamp. The microscope configuration is in the reflection mode, where the UV excitation beam is mounted above the sample surface. Thus, the illumination and imaging area take place on the same side of the specimen and the maximum fluorescence is produced in the layer and area being observed. The fluorescence emission is captured and imaged with the objective working as a condenser.[11–14]

Scanning electron microscopy (SEM) of the polymer blends was performed using a JSM-T300 microscope at two different magnifications (×350 and ×1000) with an accelerating voltage of 20 kV. Sputtering with platinum/gold alloy coated the surfaces of the polymer blends. We also obtained electron micrographs of the surface fracture using a Jeol JSM 840 microscope working with an electron beam accelerating voltage of 25 kV. The fracture surface was coated with an ~4-nm gold layer. Original magnifications of 1000× and 5000× were obtained.

Luminescence measurements at several temperatures were performed as described previously.[22] The samples were inserted into the cryosystem and kept under vacuum throughout the whole experiment. The λ_{exc} was 290 nm, which is resonant with the maximum absorption band of the naphthyl group of the P2VN homopolymer.

RESULTS AND DISCUSSION

Characterization of Homopolymers

The microstructure of PB-36 was determined by IR spectroscopy by measuring the absorbencies at 740, 912, and 967 cm^{-1}, which are assigned to cis-(1,4) units, 1,2-vinyl content, and trans-(1,4) units, respectively. The methodology involves the solution of three simultaneous equations as described elsewhere.[33] These data reveal that the PB-36 sample contains 14% vinyl groups, 50% trans units, and 36% cis units (Table I).[33]

The glass-transition temperatures (T_g) determined by DSC demonstrate that both homopolymers are totally amorphous and the T_g values for P2VN and PB-36 are about 118 and −89°C, respectively. The second DSC scan completely removes the endothermic peak present in the first scan curve [Fig. 1(a,b)]. Moreover, the thermograms for all polymer blends always exhibit two separate glass-transition temperatures that are attributed to segregated domains of both ho-

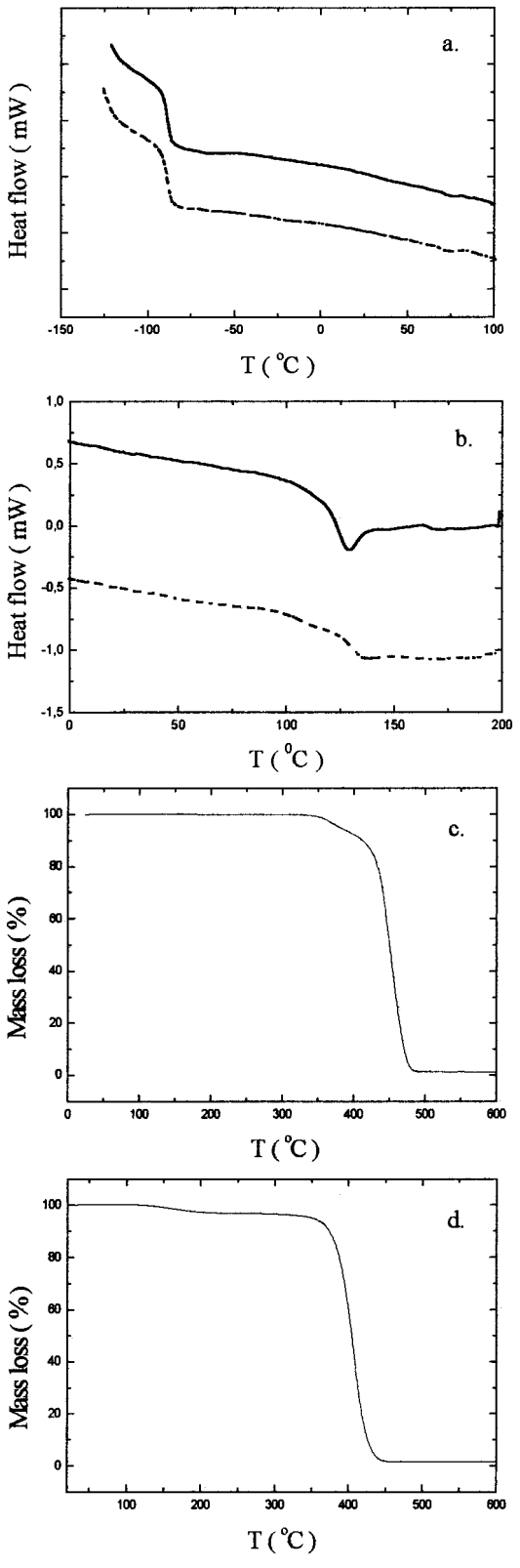

Figure 1 DSC heating thermograms for (a) PB-36 and (b) P2VN (—) first and (- - -) second scans and thermal degradation curves for (c) PB-36 and (d) P2VN. The heating rate is 10°C/min.

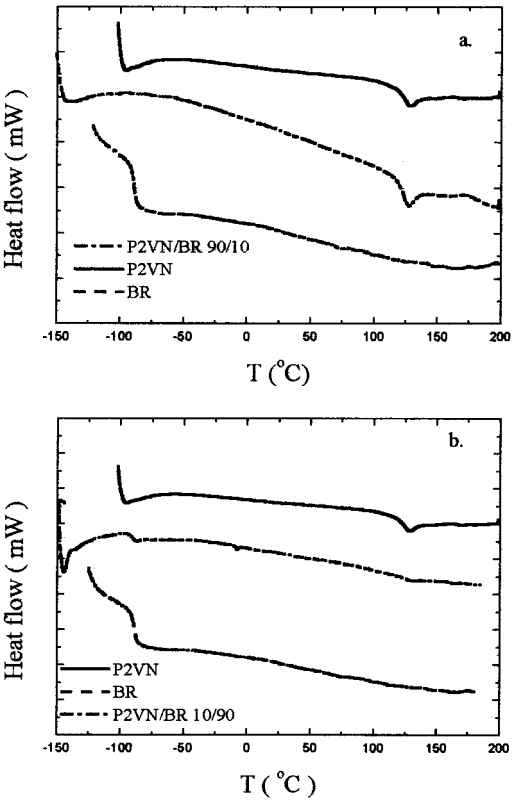

Figure 2 DSC heating thermograms (second scan) for 90% PB-36/P2VN blends corresponding to (a) a P2VN fluorescent matrix and (b) a PB-26 nonfluorescent matrix: (—) P2VN, (- - -) PB-26, and (- · -) PB-36/P2VN.

mopolymers, similar to PB/PS blends.[27,28] Nevertheless, the glass-transition temperature of blended P2VN is always higher (125°C) than that for a nonblended polymer [Fig. 2(a,b)]. There are two plausible explanations for this unexpected result: it is an apparent affect produced by the lower thermal diffusivity of the rubbery phase or it is a real shift induced by the pressure increase of the rubbery phase over the P2VN domains upon heating.[34] Additional data are necessary to explain this result.

The TGA curves for PB-36 exhibit two maximum loss rates [Fig. 1(c)]. We associate the first at ≅350°C with the evolution of butadiene and vinyl cyclohexane. The second at 453°C corresponds to main chain degradation.[35] For P2VN the TGA curve also exhibits two maximum loss rates [Fig. 1(d)] associated with the evolution of vinylic groups (157°C) and main chain degradation (428°C), analogous to thermal degradation of PS[36] (Table I).

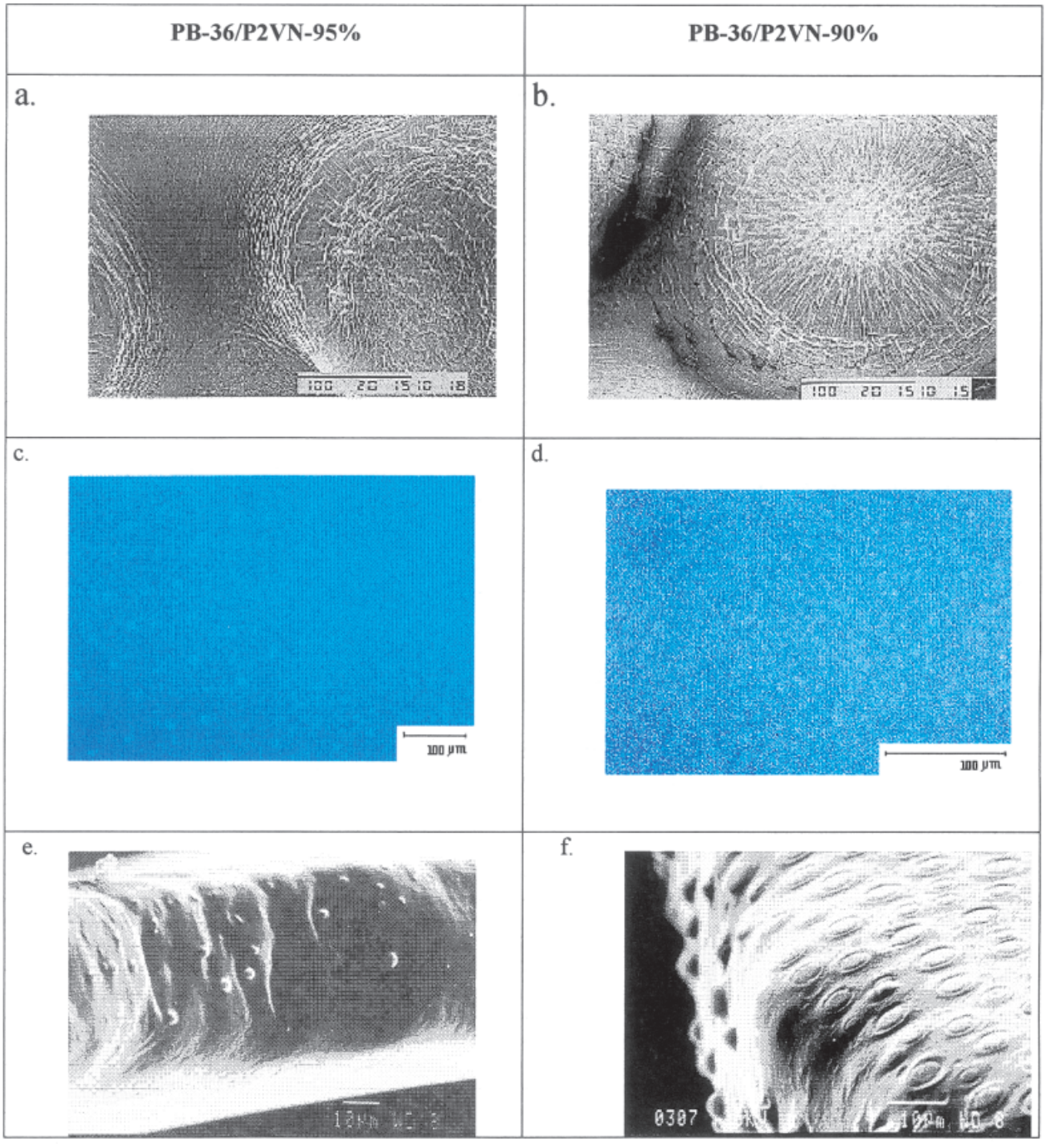

Figure 3 (a,b) SEM, (c,d) epifluorescence, and (e,f) SEM micrographs of the fracture surface for 95/5 (left) and 90/10 (right) wt % PB-36/P2VN blends showing the small isolated and fluorescent dots of P2VN dispersed in a continuous nonfluorescent PB-36 matrix. [Color figure can be viewed in the online issue, which is available at www.interscience.wiley.com.]

The weight-average molecular weight (M_w) of P2VN determined by GPC is 59,000 with a polydispersity of 2.7, and the M_w of PB-36 is 203,208 and the polydispersity of its soluble fraction is 4.1 (Table I).

Morphology of PB-36/P2VN Blends

Blends of PS and PB exhibit phase diagrams characterized by an upper critical solution temperature, a critical temperature of 23°C, and a

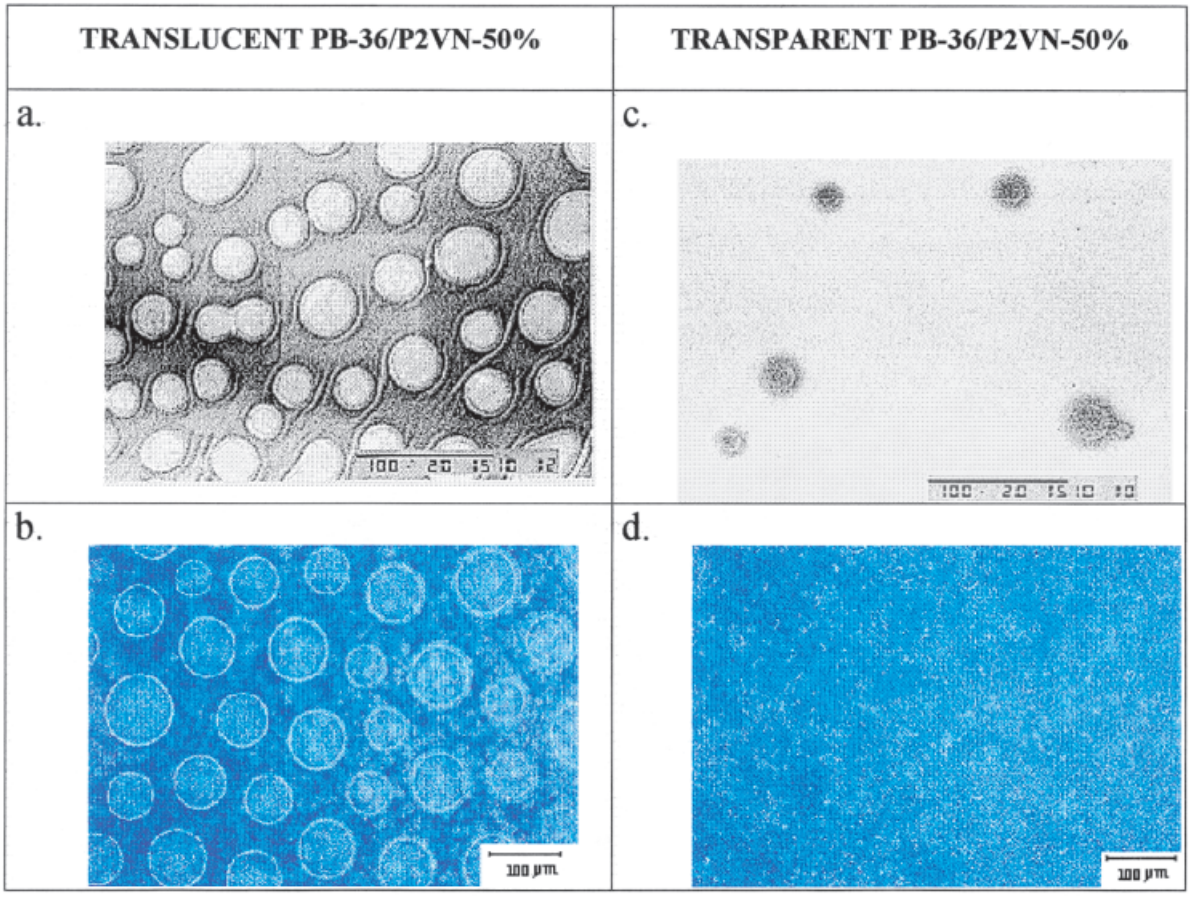

Figure 4 (a,c) SEM micrographs and (b,d) optical fluorescence micrographs of 50/50 wt % PB-36/P2VN blends showing (a,c) P2VN clusters dispersed in a continuous PB-36 matrix (translucent region) and PB-36 domains dispersed in a continuous P2VN fluorescent matrix (transparent regions). [Color figure can be viewed in the online issue, which is available at www.interscience.wiley.com.]

critical concentration of 36.9 vol % PS.[27] The structural similarity between PS and P2VN suggests similar behavior for the phase diagram of the PB-36/P2VN blends; thus, these blends must also be immiscible.

Epifluorescence microscopy is a convenient technique to analyze the morphology of PB-36/P2VN blends because P2VN is intrinsically fluorescent and can be easily visualized, but PB-36 is a nonfluorescent polymer. Thus, simultaneous to the morphology description, the micrographs also allow an *in situ* chemical analysis of the material using a nondestructive method.

The morphologies of the PB-36/P2VN blends were studied in five proportions by mass (95, 90, 50, 10, and 5 wt %) using epifluorescence, scanning electron, and SEM fracture surface microscopic techniques. It is worthy of note that the final morphology of these materials results from the sequence of events: blend preparation by casting, solvent evaporation, and subsequent annealing processes at 80°C. Regardless of the initial proportion of both homopolymers, the composition of each phase can be quite different due to phase separation.

The epifluorescence microscopy of blends with lower P2VN contents (5 and 10 wt %) reveals a dispersion of spherical isolated dots of the fluorescent polymer uniformly distributed in a nonfluorescent rubbery matrix (Fig. 3). The lack of information produced by the SEM technique is remarkable in that the micrographs show a continuous surface without discrete domains. Nevertheless, the SEM of the surface fracture confirms the presence of these droplets as spherical droplets immersed in a continuous PB-36 matrix. The relative size and the density distribution of these droplets increase with the relative increase of the amount of P2VN, and the morphology may be described as a PB-36 continuous phase with dis-

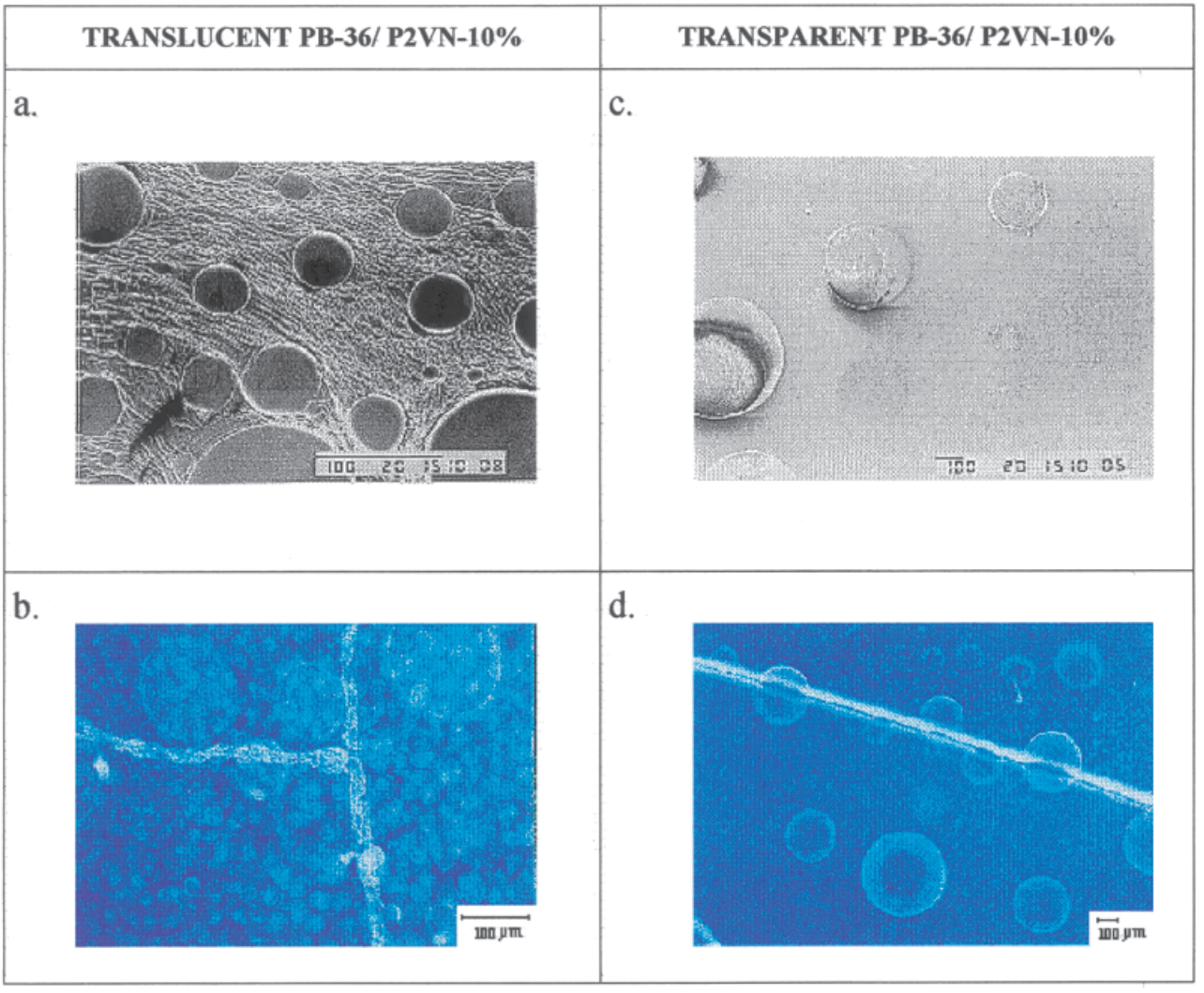

Figure 5 (a,c) SEM micrographs and (b,d) optical fluorescence micrographs of 10/90 wt % PB-36/P2VN blends showing (a,c) P2VN clusters dispersed in a continuous PB-36 matrix (translucent region) and PB-36 domains dispersed in a continuous P2VN fluorescent matrix (transparent region). [Color figure can be viewed in the online issue, which is available at www.interscience.wiley.com.]

crete P2VN domains. This type of morphology is usually obtained for systems displaying phase separation by nucleation and growth.[37,38]

The morphology of the fluorescent domains for blends with 50, 90, and 95 wt % P2VN shows larger spherical and strongly fluorescent domains (P2VN) uniformly dispersed in a matrix (PB-36) that produce a translucent region. Smaller and nonfluorescent domains of PB-36 are dispersed in a fluorescent matrix and form a transparent phase (Figs. 4–6). In addition, epifluorescence microscopy reveals that the fluorescent domains (P2VN) contain an internal microstructure formed by many tiny droplets surrounded by a fluorescent skin. However, the distribution of these droplets is higher nearer the surface compared to the central region of each domain, which shows a luminescent crown composed of aggregation (without coalescent) of fluorescent droplets. Between two crowns there is a poorly fluorescent ring characteristic of exclusion zones. The SEM micrographs of the fracture surface of one of these domains confirmed the presence of such micromorphology inside the domains [Fig. 7(a)]. The fracture also reveals that a very weak adhesion is binding the droplets to the PB-36 matrix [Fig. 7(b)].

The possibility of a two-stage phase separation process is considered to explain the presence of an internal micromorphology of the fluorescent do-

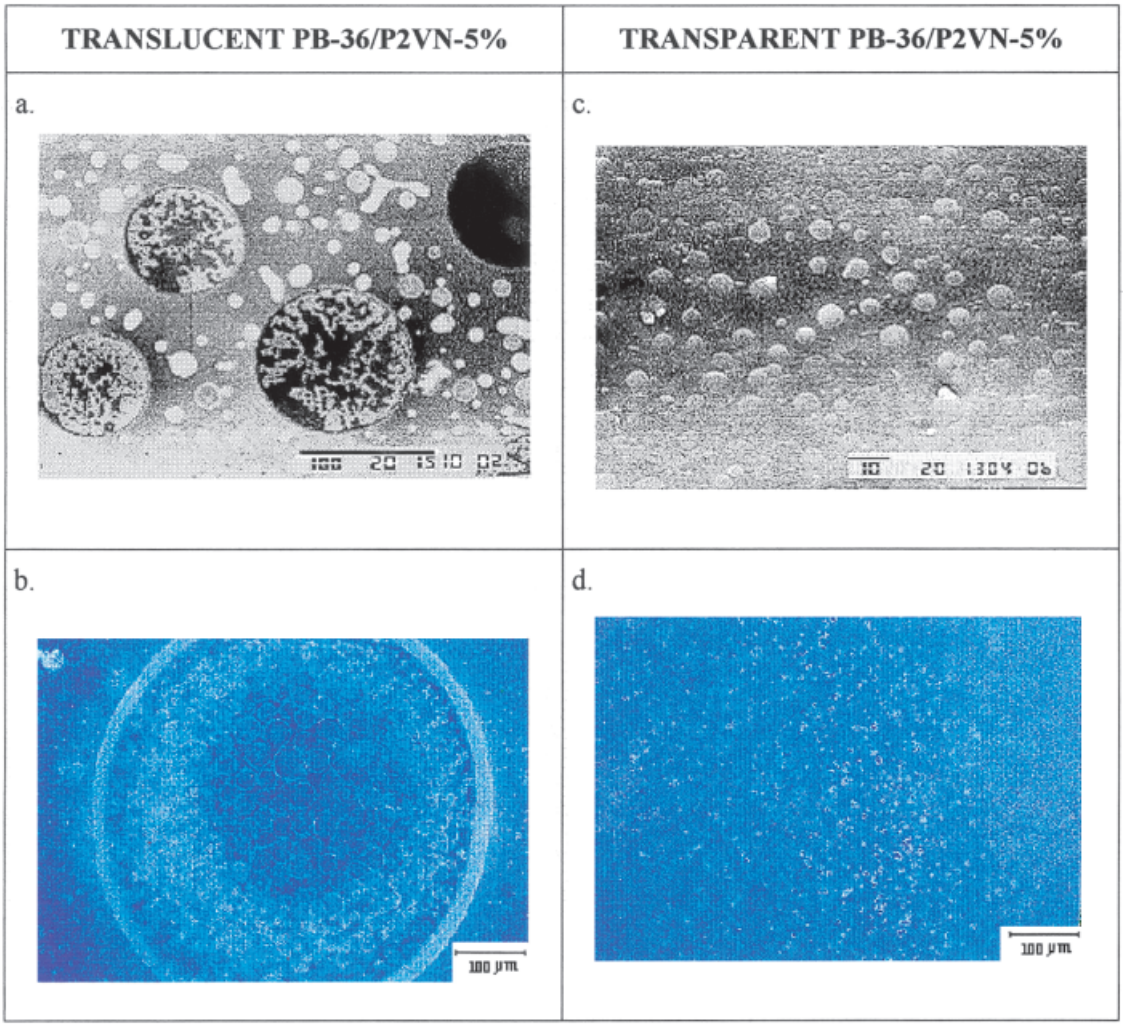

Figure 6 (a,c) SEM micrographs and (b,d) optical fluorescence micrographs of 5/95 wt % PB-36/P2VN blends showing (a,c) P2VN clusters dispersed in a continuous PB-36 matrix (translucent region) and PB-36 domains dispersed in a continuous P2VN fluorescent matrix (transparent region). [Color figure can be viewed in the online issue, which is available at www.interscience.wiley.com.]

mains. During the first separation step, the less soluble fraction is gelified in a soluble phase that produces local concentration gradients and the first step of the phase separation process. Further solvent evaporation induces a secondary phase separation inside the gelified domains that undergoes a second phase separation. The presence of spherical domains observed by either fluorescence microscopy or surface fracture using electron scanning microscopy reveals that the major contribution to the phase separation mechanism is nucleation and growth in both the primary and secondary phase separations. Thus, both steps explain the presence of spherical dispersed domains of P2VN or PB-36 in the viscous reciprocal matrix.

P2VN Fluorescence in Solid State

The fluorescence spectrum of P2VN in the solid state is composed of a structureless band centered at 400 nm that is attributed to excimer emission of the naphthyl groups.[9,10] Isolated chromophore emission, if present, is too weak to be detected and separated from the broad excimer band (Fig. 8).

A broad composed fluorescence spectra of P2VN in the solid state and a structureless band centered at 400 nm are attributed to excimer emission (Fig. 8). The isolated chromophore emission, if present, is strongly overlapped to the excimer band and was completely neglected in our analysis because the profile for the temperature

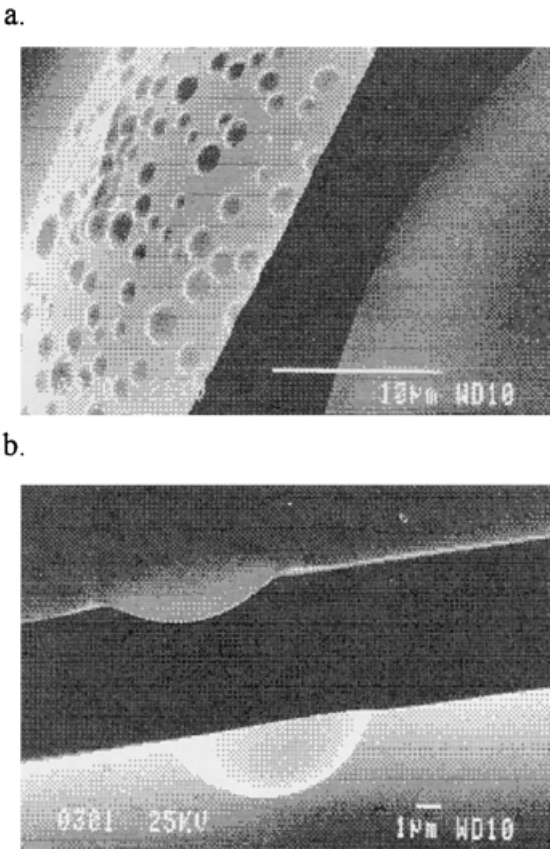

Figure 7 (a) A SEM micrograph of a fracture surface of a P2VN drop of a 5/95 wt % PB-36/P2VN blend showing (b) the weakness of the interfacial adhesion between the P2VN domain and the PB-36 matrix.

dependence of the total intensity and the intensity at 400 nm are virtually the same. The mechanism for excimer formation in P2VN is based on singlet energy migration involving both adjacent and nonadjacent chromophores, and the efficiency of the formation is controlled by the local concentration and/or mutual orientation of these chromophores and is primarily an intramolecular phenomenon.[9,10,19,39–41]

Thus, considering the small contribution of the monomer emission for the whole spectrum, the temperature dependence of the fluorescence emission was analyzed assuming that the entire spectrum is due to excimer emission and the temperature dependence of the integrated fluorescence intensity (I_F) may be analyzed by an Arrhenius-type function for the fluorescence intensity versus the reciprocal temperature:

$$\ln[(I_{F0}/I_F) - 1] = -E_a/RT \qquad (1)$$

where I_{F0} is the integrated fluorescence intensity at the lowest temperature employed, E_a is the apparent activation energy resulting from the convolution of the nonradiative deactivation of the excited state disturbed by the polymer relaxation processes, R is a gas constant, and T is the temperature. A plot of $\ln[(I_{F0}/I_F) - 1]$ versus the reciprocal of the temperature will be linear only if a unique value of the apparent activation energy is involved with the relaxation processes.[12,20–23]

Figure 9 shows the plots for the integrated fluorescence intensity versus the temperature and the corresponding Arrhenius representation of the experimental data in the temperature range of about 30–400 K during the first and second successive heating runs. The major differences are that for the first run only one linear segment was observed from 30 to 200 K with a slope change at 200 K while for the second scan two slope changes are noted, one at 110 K and the other 200 K. The apparent activation energies determined for the linear segments in the Arrhenius plots are shown in Table II. The segment between 200 and 370 K is not well represented by an Arrhenius-type function with only one apparent value of the activation energy.

The slope changes of the experimental curves are attributed to polymer relaxation processes, which are analyzed on the basis of the PS model: the lower temperature slope change (110 K) is attributed to the onset temperature of small group motions containing two or three methylene or end-naphthyl units, which are represented by a γ'-relaxation process, and the slope change at 200 ± 5 K is due to the rotation of the phenyl groups

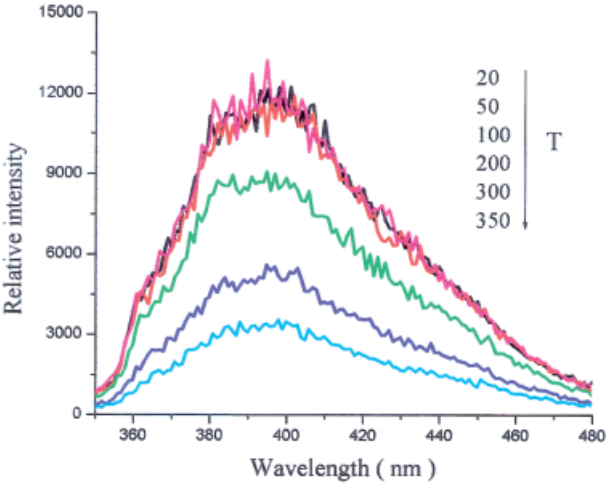

Figure 8 The typical fluorescence emission of P2VN in the solid state and in a 50/50 wt % PB-36/P2VN blend at several temperatures. [Color figure can be viewed in the online issue, which is available at www.interscience.wiley.com.]

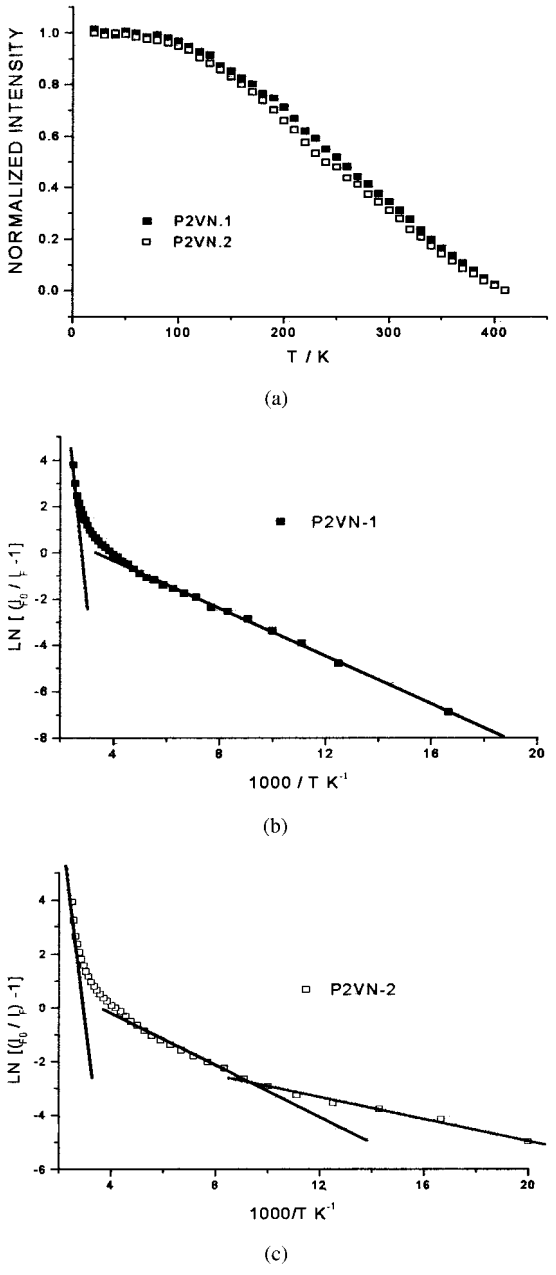

Figure 9 (a) The temperature dependence and (b,c) Arrhenius plots of the normalized and integrated fluorescence intensity of the P2VN first (-1) and second (-1) heating runs.

around the backbone chain.[42–45] Moreover, the transition at 370 ± 5 K is attributed to the onset of the local oscillation of the polymer backbone that precedes the glass transition observed calorimetrically at 390 K. The non-Arrhenius behavior observed at intermediate temperatures between 200 and 370 K reveals the complexity of the chain motions occurring in this temperature range and may involve the convolution of several radiationless pathways: the excimer formation/dissociation process and monomer deactivation by nonfluorescent mechanisms, as well the local oscillation modes of the backbone chain, which occur with PS from 320 to 350 K.[41–45]

Relaxation Processes of PB-36/P2VN

The experiments performed for the polymer blends involved the measurement of P2VN fluorescence emissions at several temperatures for the material divided into two types of zones: one that presents higher optical quality and is preferentially formed by the P2VN matrix and the other formed by the P2VN droplets dispersed in the PB-36 matrix, which is more translucent. In one case the emission is more uniform over the entire sample, which is also shown by epifluorescence microscopy, while the fluorescent droplets exhibit secondary phase separation from the other. Similar to the experiments for the P2VN homopolymer, two successive heating runs were carried out and two types of plots are constructed from the experimental data: the linear I_F versus T plot and the Arrhenius-type plot. Because for other samples the curves present similar profiles, we only show the experimental data for the heterogeneous phase of a 10% PB-36/P2VN blend in Figure 10.

A general description of the curve profiles shows that the slope change of the Arrhenius plot is more pronounced for the isolated P2VN than for the blended P2VN in either the lower or higher temperature ranges. The plots for all samples present two very well-defined onset temperatures at 220–230 and 370–380 K, and the linear representation for the temperature dependence on the Arrhenius plot suggests that they are related to only one value of the apparent activation energy. These two segments are also obtained for

Table II Relaxation Temperatures and Apparent Activation Energies for P2VN by Fluorescence Spectroscopy

	P2VN-1		P2VN-2	
Assignment	T (K)	E_a (kJ mol^{-1})	T (K)	E_a (kJ mol^{-1})
γ' Relaxation	Not observed		110	1.7
γ Relaxation	200	4.2	200	3.9
T_g	370	67	370	64

T_g (P2VN) = 390 K and T_g (PB) = 187 K, both determined by DSC; 1 and 2 represent the data for the first and second runs.

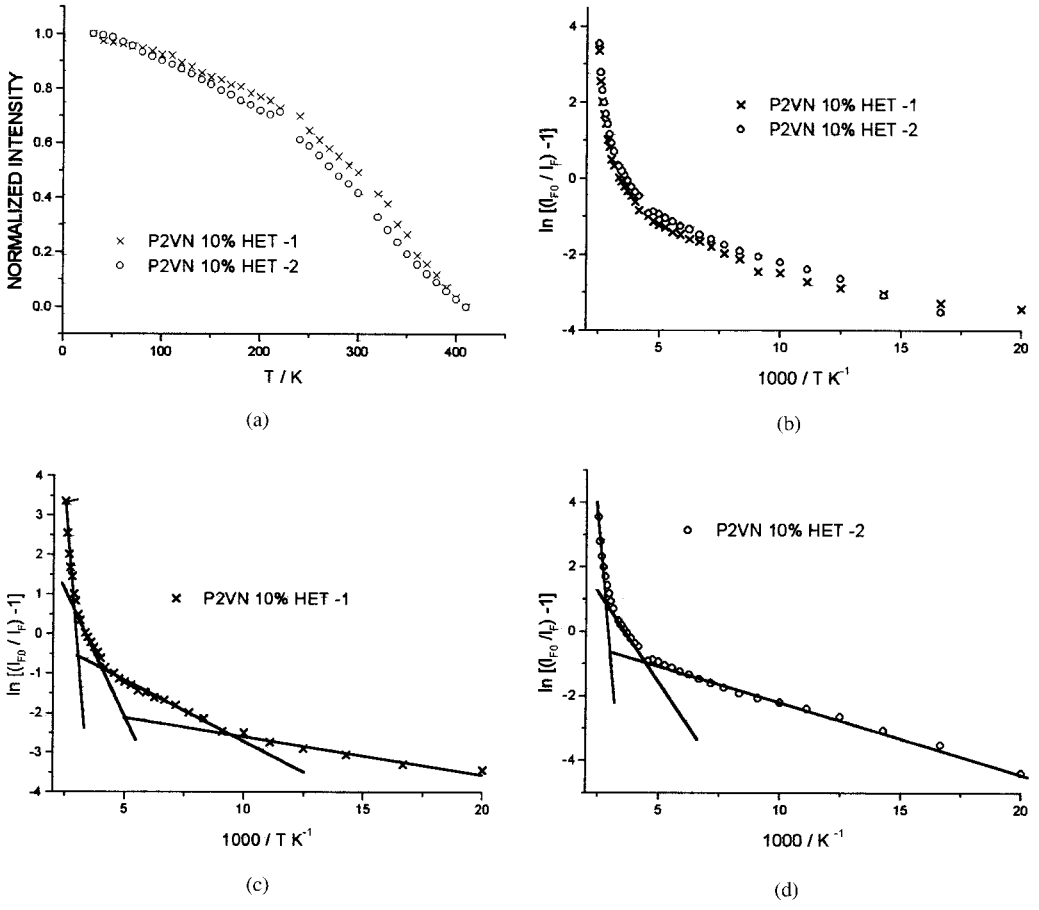

Figure 10 (a) The temperature dependence and (b) Arrhenius plot of the normalized and integrated fluorescence intensity of the 90/10 wt % PB-36/P2VN heterogeneous phase and (c,d) the linear segments simulating the relaxation processes for the first (-1) and second (-2) heating runs.

the isolated homopolymer. In addition to these two linear segments (Arrhenius-type behavior), there is a nonlinear segment in the temperature range between 230 and 370 K. Nevertheless, another segment at 290–300 K, which is absent in the homopolymer, was observed in the first run of the blended samples. These segments are only present during the first heating run and they are thus attributed to some residual stress of the sample that relaxes when the thermal history is erased. The assignments of these slope changes are based on the dependence of the fluorescence emission on the temperature of the nonblended P2VN (Table II, Fig. 9): the lower temperature is attributed to the γ'-relaxation process due to the movements of short segments of the P2VN chains; the onset temperature at 200–230 K is attributed to the rotation of naphthyl groups around the polymer backbone; and the relaxation processes at 370–380 K are assigned to the glass transition in the P2VN phase.

It is worthy of note that the slope change at 200–230 K is always well defined for the second heating run and depends on the morphology and the composition of the polymer blends. For samples where P2VN is the matrix and PB-36 is the discrete phase, the onset temperature is observed at 200 K; for samples where the P2VN is the discrete phase, their segment is observed at higher temperatures (ca. 230 K). Although the explanation for this behavior cannot be established using the present data, it seems to not be fortuitous because the glass-transition temperature is also observed at higher temperatures for the same type of sample.

CONCLUSIONS

In this work PB-36/P2VN polymer blends were prepared in film form by casting a solution con-

taining both homopolymers. Because the system is immiscible, there is phase separation in the later stages of solvent evaporation, leading to the formation of discrete and spherical domains dispersed in a continuous matrix. In addition, because the viscosity of the medium increases with solvent evaporation, the coalescence of these domains is inhibited and the morphology is partially defined by the course of the solvent evaporation. Although the annealing process eliminates the material stress and equilibrates the samples, it does not lead to the most stable morphology because the temperature is lower than the P2VN glass transition to prevent PB crosslinking.

Epifluorescence microscopy allows identification of the fluorescent P2VN phase either when this polymer is forming discrete domains in the PB-36 matrix or when it is the continuous phase. Furthermore, this technique unequivocally reveals that dispersed droplets rich in P2VN exhibit an internal micromorphology that results from a secondary phase separation process. Indeed, fracture surface electron microscopy confirms the presence of a secondary morphology inside the spherical and discrete domains.

The Arrhenius-type function represents the kinetic behavior of the excimer fluorescence emission for temperatures below relaxation (involving short segments of the polymer chain) and above the glass transition, but it fails in the intermediate temperature range. Although we are not able to explain the reason for this at present, we may assume that the major reason is the convolution of several kinetic pathways involved with chain motions above 200–230 K.

We thank FAPESP for financial support. The authors also thank Prof. Inés F. de Piérola (UNED, Spain) and Prof. Carol Collins for useful discussions.

REFERENCES

1. Spontak, R. J.; Williams, M. C.; Agard, D. A. Macromolecules 1988, 21, 1377.
2. Anastasiadis, S. H.; Russell, T. P.; Satija, S. K.; Majkrzak, C. F. J Chem Phys 1990, 92, 5677.
3. Søndergaard, K.; Lyngaae-Jørgensen, J. Polymer 1996, 37, 509.
4. Nam, K. H.; Jo, W. H. Polymer 1997, 36, 3727.
5. (a) Henderson, C. P.; Williams, M. C. Polymer 1985, 26, 2021; (b) Henderson, C. P.; Williams, M. C. Polymer 1985, 26, 2026.
6. Chen, C.-T.; Morawetz, H. Macromolecules 1989, 22, 159.
7. Granados, E. G.; González-Benito, J.; Baselga, J.; Dibbern-Brunelli, D.; Atvars, T. D. Z.; Esteban, I.; Piérola, I. F. J Appl Polym Sci, to appear.
8. Morawetz, H. Pure Appl Chem 1980, 52, 277.
9. Semerak, S. N.; Franck, C. W. Macromolecules 1984, 17, 1148.
10. Gashgari, M. A.; Frank, C. W. Macromolecules 1981, 14, 1558.
11. Pierola, I. F.; Atvars, T. D. Z.; Salom, C.; Prolongo, M. G. In Polymer–Polymer Interactions: Fluorescence Studies, Polymeric Materials Encyclopedia; Salamone, J. C., Ed.; CRC Press: Boca Raton, FL, 1996; Vol. 8, p 6362.
12. Dibbern-Brunelli, D.; Atvars, T. D. Z. J Appl Polym Sci 1995, 58, 779.
13. Dibbern-Brunelli, D.; Atvars, T. D. Z.; Joekes, I.; Barboza, V. C. J Appl Polym Sci 1998, 69, 645.
14. Dibbern-Brunelli, D.; Atvars, T. D. Z. J Appl Polym Sci 1995, 55, 889.
15. Bokobza, L.; Pham-Van-Cang, C.; Monnerie, L.; Vandendriessche, J.; De Schryver, F. C. Polymer 1989, 30, 45.
16. Gashgari, M. A.; Franck, C. W. Macromolecules 1981, 14, 1558.
17. Klopffer, M.-H.; Bokobza, L.; Monnerie, L. Polymer 1998, 39, 3445.
18. Klopffer, M.-H.; Bokobza, L.; Monnerie, L. Makromol Symp 1997, 119, 119.
19. Jing, D. P.; Bokobza, L.; Monnerie, L.; Collart, P.; De Schryver, F. C. Polymer 1990, 31, 312.
20. Ye, J. Y.; Hattori, T.; Nakatsuka, H. Phys Rev B 1997, 56, 5286, and references therein.
21. Winnik, M. A., Ed. Photophysical and Photochemical Tools in Polymer Science: Conformation, Dynamic and Morphology, NATO ASI Series; Riedel: Dordrecht, The Netherlands, 1986; Vol. 183.
22. Christoff, M.; Atvars, T. D. Z. Macromolecules 1999, 32, 6101, and references therein.
23. Talhavini, M.; Atvars, T. D. Z.; Schurr, O.; Weiss, R. G. Polymer 1998, 39, 3221.
24. Atvars, T. D. Z.; Dorado, A. P.; Pierola, I. F. Polym Networks Blends 1997, 7, 111.
25. Kim, S.; Yu, J.-W.; Han, C. C. Rev Sci Instrum 1996, 61, 3940.
26. Mark, H. F., Bikales, N. M., Overberger, C. G., Menges, G., Eds. Encyclopedia of Polymer Science and Technology; Wiley: New York, 1989; Vol. 16, p 88.
27. Danchinov, S. K.; Shilanov, Y. D.; Godovsky, Yu. K. Macromol Symp 1996, 112, 69.
28. Chu, L.-H.; Guo, S.-H.; Chiu, W.-W.; Tseng, H.-C. J Appl Polym Sci 1993, 49, 1791.
29. Xi, K.; Krause, S. Macromolecules 1998, 31, 3974.
30. Han, C. D.; Chun, S. B.; Hahn, S. F.; Harper, S. Q.; Savickas, P. J.; Meunier, D. M.; Li, L.; Yalcin, T. Macromolecules 1998, 31, 394.
31. Roe, R.-J.; Zin, W.-C. Macromolecules 1980, 13, 1221.
32. Hill, R. G.; Tomlis, P. E.; Higgins, J. S. Polymer 1985, 26, 1708.

33. Frankland, J. A.; Edwards, H. G. M.; Johnson, A. F.; Lewis, I. R.; Poshyachinda, S. Spectrochim Acta 1991, 47A, 1511.
34. DiMarzio, E. A.; Gibbs, J. H.; Fleming III, P. D.; Sanchez, I. C. Macromolecules 1976, 9, 763.
35. Brazier, D. W.; Schwartz, N. V. J Appl Polym Sci 1978, 22, 113.
36. Yang, M.; Shibasaki, Y. J Polym Sci Part A: Polym Chem 1998, 36, 2315.
37. Heier, J.; Kramer, E. J.; Revecz, P.; Battisitig, G.; Bates, F. S. Macromolecules 1999, 32, 3758.
38. Oyanguren, P. A.; Galante, M. J.; Andromaque, K.; Frontini, P. M.; Williams, R. J. J Polym 1999, 40, 5249.
39. Pálszegi, T.; Sokolov, I. M.; Kauffmann, H. F. Macromolecules 1998, 31, 2521.
40. Vala, M. T., Jr.; Silbey, R.; Rice, S. A.; Jortner, J. J Chem Phys 1961, 41, 2846.
41. Sienicki, K.; Mattice, W. L. Macromolecules 1989, 22, 2854.
42. Yano, O.; Wada, Y. J Polym Sci A 1971, 669.
43. Kawaguchi, T.; Kanaya, T.; Kaji, K. Physica B 1995, 213/214, 510.
44. Nakatani, H.; Nitta, K.; Soga, K. Polymer 1998, 39, 4273.
45. Havránek, A.; Pospísil, J.; Buriánek, J.; Honskus, J.; Nedbal, J. Progr Colloid Polym Sci 1988, 78, 17.